Structure of nonlinear traveling-wave states in finite geometries

M. C. Cross
California Institute of Technology, Pasadena, California 91125
(Received 9 November 1987)

Numerical simulation of coupled amplitude equations is used to investigate the effect of the wave propagation on the one-dimensional spatial structure of nonlinear wave states in finite geometries. The work is motivated by experiments on oscillatory convection in binary fluid convection. Predictions of confined states, temporally modulated confined states, and other dynamic states are discussed and compared with experiment.

I. INTRODUCTION

Considerable progress has been made in the study of pattern formation in driven dissipative systems which have an instability to a stationary state with spatial periodicity. Recently flow visualization experiments on Rayleigh-Bénard convection in binary fluid mixtures, where the first instability is to an oscillatory spatially periodic state, have stimulated the investigation of similar questions in a dynamic context. In this paper I will discuss the effect of the propagation on the spatial structure expected in finite one-dimensional geometries, using the amplitude equation formalism to describe the slow space and time modulation of the basic pattern. This approach has some generality, but I will make particular reference to experiments on binary fluid convection.

Nonlinear wave states may, depending on the system parameters, develop side band instabilities to spatially inhomogeneous states. This instability is known as the Benjamin-Feir instability.[1] Numerical simulations[2] suggest these unstable states may have complex spatial and temporal behavior. It is tempting to ascribe any spatial inhomogeneity or nonperiodic time dependence observed in experiment to this mechanism. The present work shows that in finite geometries with realistic boundary conditions the simple fact that the waves propagate can lead to spatial inhomogeneity and nonperiodic dynamics, unexpected from our experience with the stationary case, even when the Benjamin-Feir instability is completely absent. There is reason to believe that the nonlinear saturated state in binary fluid convection, which usually has a rather low frequency compared with the linear onset frequency,[3] will show rather weak Benjamin-Feir tendencies: such effects would be expected to scale with the basic frequency. Thus the mechanisms proposed in the present work may well be responsible for the behavior observed. A comparison with experiment will be made in Sec. V. Unfortunately, a detailed comparison cannot be made since the nonlinear saturated state is not well understood in this system. Thus the predictions must be taken only as indicative of the phenomena that may occur. There may well be other important physics that serves to reinforce or nullify the effects predicted by the simple description. In particular the very long relaxation times due to the small concentration diffusion coefficient in typical binary fluid systems may have important consequences.

The basic question addressed in this paper can be thought of as asking for the implications of the phenomenon known as convective instability when finite but large geometries with realistic boundary conditions are considered. Deissler[4] has recently studied convective instabilities in Ginzburg-Landau equations like the ones used below: due to the propagation of the waves an initial perturbation of an unstable quiescent state may propagate away sufficiently fast that *at the position of the initial perturbation* the perturbation dies away although at a position $x = vt$ with v some velocity the perturbation grows. For the Ginzburg-Landau equations this phenomenon occurs when the dimensionless propagation velocity s exceeds 2. In finite geometries I do indeed find a change of behavior around this value.

In a previous paper[5] I predicted that for $s \gtrsim 2$ the nature of the steady solution in finite geometries changed to one in which the waves reached their saturated value only in some fraction of the box, leaving the other portion in the "unstable" quiescent state. (A small amplitude disturbance in the quiescent region grows, but also travels to the saturated region, leaving the small amplitude region unaffected.) Such states were observed[6,7] in experiments on binary fluid convection, and called "confined states"—although there is no firm proof that the observations are related to the mechanism I proposed.

In the present paper I discuss the prediction of the confined states in more detail, and then describe additional possibilities. In particular I also discuss defect states, temporally modulated confined states, quasiperiodic states in which the system oscillates between states of large amplitude right-moving waves in the right half of the cell to large amplitude left-moving waves in the left half of the cell, and symmetric nonlinear peridoic states reminiscent of the symmetric linear transients[8] accounted for in Ref. 5.

The plan of the paper is as follows. In Sec. II I discuss the amplitude equation formalism used, and the restrictions of its applicability to small propagation speeds. Section III describes defect states and confined states found in the numerical solution for stationary solutions to the amplitude equations. In Sec. IV dynamic solutions

are discussed. Comparison with experiment on binary fluid convection is made in Sec. V.

II. AMPLITUDE EQUATIONS

Near the instability to an oscillatory, spatially periodic state with symmetry $x \rightarrow -x$ the system can be described in terms of complex equations for the amplitudes A_R and A_L of right- and left-moving waves, i.e.,

$$\mathbf{V}(x,z,t) \simeq \mathbf{V}_0(z)[\, A_R(x,t)e^{ik_c x} + A_L(x,t)e^{-ik_c x}]e^{-i\Omega_c t} + \text{c.c.} \,, \quad (1)$$

where $\mathbf{V}$ is the vector of variables defining the state at the point (x,z) (e.g., fluid velocity, temperature, and concentration in binary fluid convection), and the coordinate z represents the fast transverse coordinates (e.g., the vertical coordinate spanning the distance between the plates in Rayleigh-Bénard convection). The vector $\mathbf{V}_0(z)$ is the eigenvector of the linear instability problem at threshold with zero growth rate, k_c is the threshold wave number minimizing the onset driving, and Ω_c is the frequency of the oscillations here.

In general, the equations for the slow one-dimensional space and time modulations of the basic waves takes the form[9]

$$\begin{aligned}\tau_0(\partial_t + s\partial_x)A_R &= \epsilon(1+ic_0)A_R + (1+ic_1)\xi_0^2\partial_x^2 A_R \\ &\quad - g_1(1+ic_2)|A_R|^2 A_R - g_2(1+ic_3)|A_L|^2 A_R \,, \end{aligned} \quad (2)$$

$$\begin{aligned}\tau_0(\partial_t - s\partial_x)A_L &= \epsilon(1+ic_0)A_L + (1+ic_1)\xi_0^2\partial_x^2 A_L \\ &\quad - g_1(1+ic_2)|A_L|^2 A_L - g_2(1+ic_3)|A_R|^2 A_L \,, \end{aligned}$$

with ϵ the control parameter [e.g., $(R-R_c)/R_c$ with R the Rayleigh number and R_c its threshold value] and $\tau_0, s, \epsilon, g_1, g_2, c_0, c_1, c_2, c_3$ real parameters to be determined from the basic equations.

Notice that due to the first spatial derivative the small parameter ϵ cannot be entirely eliminated from Eqs. (1) and (2) by scale changes of A, x, and t: the expansion is not uniform in the parameter ϵ. In the standard derivation[10] of a *single* amplitude equation, for example for right-moving waves, a coordinate moving with the group speed s is introduced

$$\bar{x} = x - st \,. \quad (3)$$

The equation can then be rescaled to give

$$\begin{aligned}\partial_T A_R &= (1+ic_0)A_R + (1+ic_1)\partial_X^2 A_R \\ &\quad - (1+ic_2)|A_R|^2 A_R \\ &\quad - g(1+ic_3)|A_L|^2 A_R \end{aligned} \quad (4)$$

with $X = \epsilon^{1/2}\bar{x}/\xi_0$, etc., with no small parameters remaining.

This transformation to a moving coordinate system is not useful in studying the state in a stationary fixed geometry, or a mixed state of both right- and left-moving waves. In these situations, a direct solution of Eqs. (1) and (2) can lead to results with spatial variations on a length scale $O(1)$, not the long length scale assumed in the derivation of the equations. A simple balance of the terms in Eqs. (1) and (2) leads to the characteristic lengths $\xi_L \sim (s/\epsilon)\tau_0$ and $\xi_S = (s^{-1})\xi_0^2/\tau_0$. The short length scale ξ_S is typically involved for waves *approaching* a rigid boundary or each other (Fig. 1). Such solutions are inconsistent with the derivation of Eqs. (1) and (2) and cannot be truested as accurately describing the real fluid behavior.

We are familiar with the fact that the original microscopic equations may have a different, rapid spatial variation near sidewalls in stationary Rayleigh-Bénard convection.[11] However, the rapid variation occurs in the region near the sidewall where the amplitudes are small, and can easily be treated exactly in a linear theory. The solution is matched to a *slowing* varying amplitude function, which then connects to the nonlinear regions according to the amplitude equation. In the situation we are discussing here, the rapid spatial variation and nonlinear regions overlap, and the simple matching procedure, depending on the separation of these regions, will no longer work.

In the absence of suitable schemes to solve this problem I have chosen instead to consider a particular regime where these effects disappear. Since the short length scale comes from the compression due to the propagation, I consider situations where propagation effects are small compared with the usual saturation and diffusion effects, which essentially corresponds to the frequency of

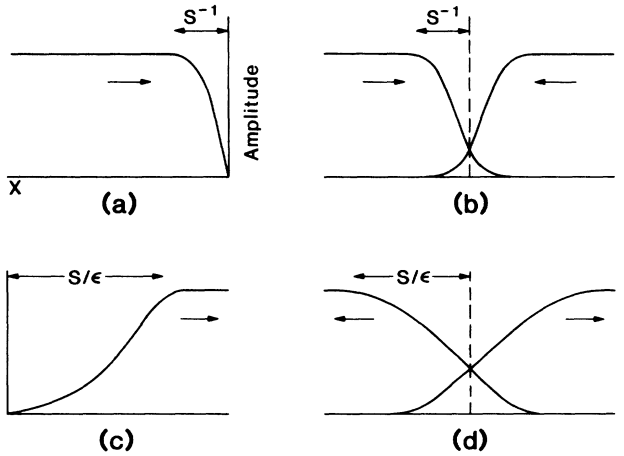

FIG. 1. Schematic diagrams of the healing of the amplitude for group speed s of order unity: (a) waves approaching a sidewall, (b) waves approaching each other (a shock); (c) waves moving away from a sidewall, (d) waves leaving a source (target). In (a) and (b) the short healing length $\xi_S \sim s^{-1}$ is involved, and an amplitude equation calculation will not be accurate for $s = O(1)$.

the waves being small. In this case s becomes small, and the other dispersive parameters c_0, c_1, c_2, c_3 may be set to zero. Formally, we perform the rescaling $X=\epsilon^{1/2}x/\xi_0$, $T=\epsilon t/\tau_0$, $\bar{s}=s\epsilon^{-1/2}\tau_0/\xi_0$, $\bar{A}_{R,L}=\epsilon^{-1/2}g_1^{1/2}A_{R,L}$, and $g=g_2/g_1$ to give

$$(\partial_T+\bar{s}\partial_X)\bar{A}_R=\bar{A}_R+\partial_X^2\bar{A}_R-(|\bar{A}_R|^2+g|\bar{A}_L|^2)\bar{A}_R\ , \tag{5}$$

$$(\partial_T-\bar{s}\partial_X)\bar{A}_L=\bar{A}_L+\partial_X^2\bar{A}_L-(|\bar{A}_L|^2+g|\bar{A}_R|^2)\bar{A}_L\ , \tag{6}$$

and consider $\bar{s}$ to be $O(1)$ [i.e., s is $O(\epsilon^{1/2})$ and small in the original units].

There is additional motivation for studying Eqs. (5) and (6) at this stage. The full behavior of Eqs. (1) and (2) is in general very complicated, with Benjamin-Feir instabilities leading to complex time dependence. It seems advisable to first isolate the effect of the translation of the basic patterns by the group velocity s, and to see if experiment may be accounted for on this basis, before invoking the full complexity of Eqs. (1) and (2).

There is also more physical motivation from the experiments on binary fluid convection. The Hopf bifurcation there is apparently inverted (subcritical) for most values of the fluid parameters, and Eqs. (1) and (2) are not directly useful. However, empirically[3] the system often saturates in a nonlinear state with properties rather well characterized by the stationary state expected for pure fluid convection, except for a *slow* translation of the rolls. Phenomenologically we might attempt to describe such a state by Eqs. (5) and (6). The parameters ξ_0, τ_0 would be given by results for pure, stationary convection, and ϵ would be taken to be $(R-R_{cp})/R_{cp}$ with R_{cp} the critical Rayleigh number for pure stationary convection (Fig. 2). Clearly Eqs. (5) and (6) are an oversimplification. The actual structure of the solution will involve boundary layers coming from the concentration diffusion and depending on the strength of the flow, so that the parameters such as s will probably be amplitude dependent, and the whole structure will change for very small amplitudes. Using the equations with fixed parameters everywhere, even where the amplitudes become small, may be too naive. Nevertheless, studying the equations may well give a useful indication of the type of phenomena to be expected. A full description must clearly depend on a better understanding of the nonlinear saturated state.

A second region where propagation effects become weaker is approaching the codimension-2 point where the oscillatory instability collides with the stationary instability, and the frequency Ω_c goes to zero. In binary fluid convection this point is reached by tuning the separation ratio ψ. Again the phenomenon is complicated by the small value of the Lewis number L (the ratio of concentration to thermal diffusivities), typically 10^{-2} to 10^{-3}. In the region $-\psi\sim L^2$ a degenerate amplitude equation must be used. For $1\gg -\psi\gg L^2$ the frequency becomes small, but the expansion about the codimension-2 point is no longer valid. Equations (5) and (6) should be a useful description in this region, providing the time scale of the motion is slow compared to Ω_c^{-1}.

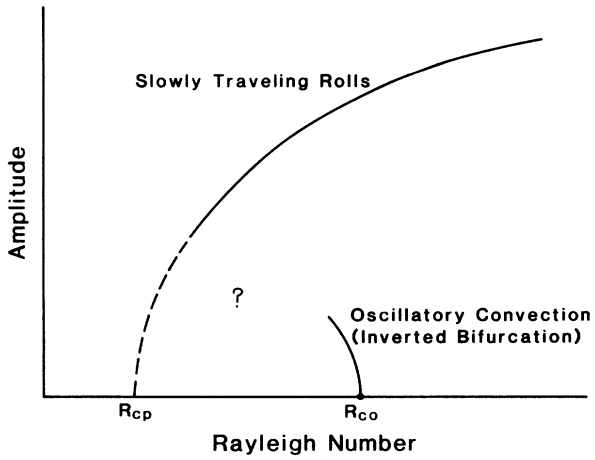

FIG. 2. Schematic diagram of possible behavior of binary fluid convection suggested by the experiments of Ref. 3. The amplitude of the slowly traveling rolls appears close to that expected for stationary convection in the corresponding pure fluid given by putting ψ to zero. This breaks down for small amplitudes $R\to R_{cp}$ indicated by the dashed line, and the curve for the finite amplitude traveling state presumably connects to the inverted bifurcation point for oscillatory convection, but in a way that has not yet been calculated.

Finally, it might be hoped that the results based on Eqs. (5) and (6) give a qualitative indication of the effect of the translation on the solutions even in more general situations such as spiral waves in Taylor-Couette flow,[12] or binary fluid convection away from the codimension-2 point.

In a finite geometry we must also consider boundary conditions on Eqs. (1) and (2). If the amplitudes become small near the boundaries we expect linear homogeneous boundary conditions, which are restricted by symmetry arguments to the form

$$\begin{aligned} &A_R-\alpha_\pm\partial_x A_R-\beta_\pm\partial_x A_L=0\ ,\\ &A_L-\alpha_\pm^*\partial_x A_L-\beta_\pm^*\partial_x A_R=0\ , \end{aligned} \tag{7}$$

for $x=(\frac{1}{2}\pm\frac{1}{2})l$ with $\alpha_+=-\alpha_-^*=\alpha$ and $\beta_+=-\beta_-^*=\beta$ expected to be $O(1)$. For the scaled equations the boundary conditions at $X=\bar{l}=\epsilon^{1/2}l$ will take the same form as (7) with $A_{R,L}\to\bar{A}_{R,L}$, $x\to X$, and $\alpha,\beta\to\bar{\alpha},\bar{\beta}$ with $\bar{\alpha}=\epsilon^{1/2}\alpha/\xi_0$ and $\bar{\beta}=\epsilon^{1/2}\beta/\xi_0$. Note $\bar{\alpha}$ and $\bar{\beta}$ are both small for small ϵ: we will consider them as small numbers, but not necessarily scaling with $\epsilon^{1/2}$. In this limit the reflection coefficient[5] of linear waves described by Eqs. (5) and (6) is $r=-\bar{\beta}^*\bar{s}$.

For convenience we bring together the scaled equations, we use

$$(\partial_t+s\partial_x)A_R=A_R+\partial_x^2A_R-(|A_R|^2+g|A_L|^2)A_R\ , \tag{8}$$

$$(\partial_t-s\partial_x)A_L=A_L+\partial_x^2A_L-(|A_L|^2+g|A_R|^2)A_L\ , \tag{9}$$

$$A_R - \alpha_{\pm}\partial_x A_R - \beta_{\pm}\partial_x A_L = 0 ,$$
$$A_L - \alpha_{\pm}^{*}\partial_x A_L - \beta_{\pm}^{*}\partial_x A_R = 0 , \tag{10}$$

for $x = (\frac{1}{2} \pm \frac{1}{2})l$ with $\alpha_+ = -\alpha_-^* = \alpha$ and $\beta_+ = -\beta_-^* = \beta$. All the bars, etc. have been dropped: the relevant scalings with ϵ are to be understood in going back to the original variables.

The value $s = 2$ is expected to play a special role dividing different classes of behavior. This can be seen by considering the stability of the quiescent state ($A_R = A_L = 0$) towards a single wave $A_R \neq 0$ in an infinite region. In this region we can transform to a frame moving with speed s, when Eq. (8) reduces to the complex Fisher equation. It is known[13] that real, localized initial conditions will lead to outwardly propagating fronts with asymptotic speed 2, and Ben-Jacob *et al.*[14] suggest the same result is almost certainly true for localized complex initial conditions. Transforming back to the original frame we see that for $s > 2$ a local perturbation at some $x = x_0$ will eventually decay locally (i.e., at x_0) although it will grow to saturation at $x = vt + x_0$, with $s - 2 < v < s + 2$. On the other hand, for $s < 2$ the perturbation will grow at x_0. The implications of this simple idea in a large but finite region are the main focus of this paper.

In a finite geometry it is useful to consider the important length scales. As we have seen Eqs. (8) and (9) lead to characteristic healing lengths for the amplitudes $\xi_L \sim s, \xi_S \sim s^{-1}$. In addition, we have the length of the system l, and the characteristic length[5] observed in the linear regime $\lambda^{-1} \sim l/|\ln(r)|$. We will assume l is always large compared to ξ_S, so that the latter is not an important length. The important parameters are s and then l/s. In particular the linear onset is given by $\lambda^{-1}/s \sim 1$ or $l/s \sim |\ln r|$, describing the balance between exponential growth during the propagation across the cell, and the reduced amplitude due to reflection at the boundaries.

III. STATIONARY SOLUTIONS

Statinary solutions of Eqs. (8)–(10), corresponding to simply periodic solutions of the original equations, were constructed using a finite difference Newton-Raphson procedure. Note that temporally unstable solutions may well be produced by this method: the stability to small perturbations is studied using the full dynamic solution described below.

There are two main results: the transition between solutions that fill the cell for $s \lesssim 2$, and solutions that are large only in part of the cell for $s \gtrsim 2$ (the confined states); and the existence of defect solutions in large enough cells. The former was described in a previous brief publication:[5] the latter has also been investigated by Coullet *et al.*[15]

A. Confined states

The transition between filling and confined states is illustrated in Fig. 3. For $s < 2$ a typical solution is shown in the top part of the figure. (Defect solutions may also be found, and are described below.) Notice the predominance of one set of waves—here the ones moving to positive x—with a small reflected amplitude of the left moving waves at $x = l$ that is suppressed in the bulk by the nonlinearity. An alternative solution with the role of left- and right-moving waves reversed may also be found. In either case traveling waves are apparent over most of the length, except for short healing lengths $\xi_{\pm}$ near the ends of the cell that are independent of l. If l is increased, the fraction of the cell filled with saturated waves increased as would be expected from the estimate $1 - (\xi_+ + \xi_-)/l$ (Fig. 4).

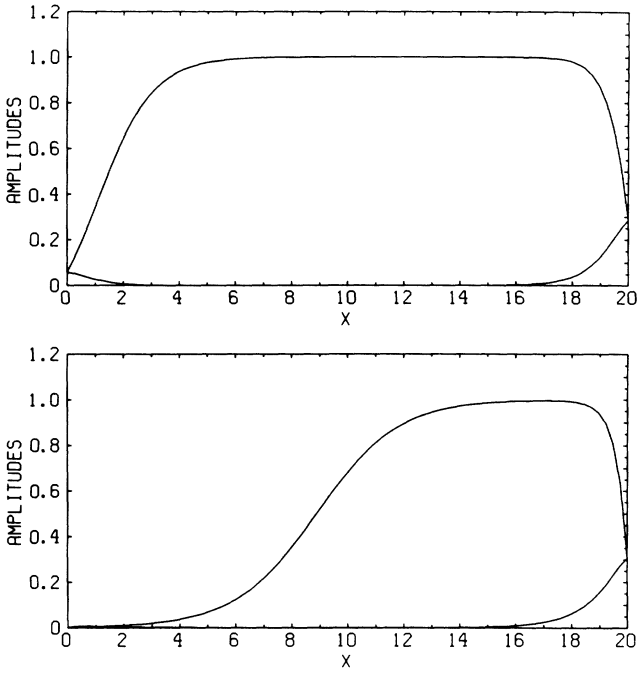

FIG. 3. Comparison of the amplitudes $A_R(x)$ and $A_L(x)$ in stationary solutions of Eqs. (8)–(10) for $s < 2$ (upper figure) and $s > 2$ (lower figure). In both cases the right-moving wave A_R is dominant. The parameters used are $l = 20, g = 4$ with $s = 1.0$, $\alpha = \beta = -0.30$ in the upper figure, and $s = 2.2, \alpha = \beta = -0.18$ in the lower figure.

For $s \gtrsim 2$ the situation is quite different as shown in the lower part of Fig. 4. In large boxes stationary solutions exist, but the reflected A_L wave, exponentially suppressed in the region of saturated A_R and then reflected at $x = 0$, is clearly needed to reexcite the A_R wave. (I describe the situation in Fig. 3; the inverse solution may also be found.) The magnitude of $A_{R,L}$ at $x = 0$ decreases as l is increased, and the length over which A_R is small roughly scales with the size of the system (Fig. 4). Balancing the exponential decay of A_L over the region l_R where A_R is saturated, with the exponential growth over the region $l - l_R$ gives the estimate for large l (when the reduction in amplitudes by reflection effects is negligible)

$$\frac{l_R}{l} \simeq \frac{[s^2 + 4(g-1)]^{1/2} - s}{[s^2 + 4(g-1)]^{1/2} + s - 2[s^2 - 4]^{1/2}} . \tag{11}$$

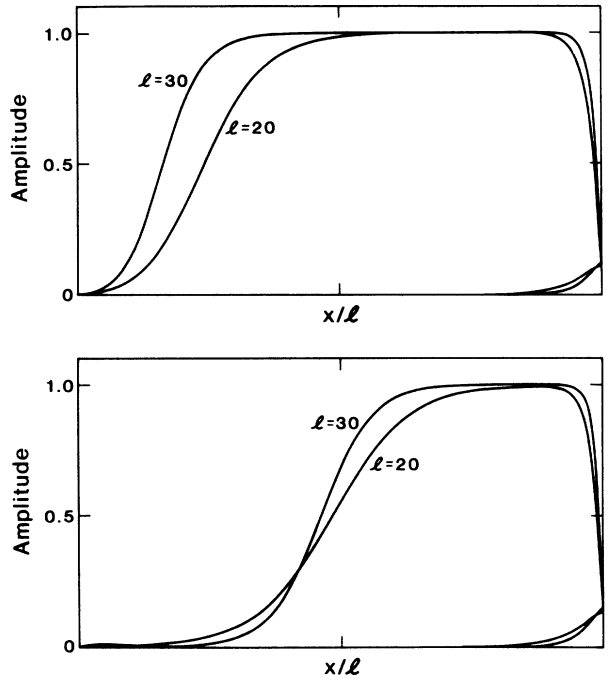

FIG. 4. Contrasting behavior for $s<2$ (upper figure) and $s>2$ (lower figure) of the amplitudes $A_R(x)$ and $A_L(x)$ of right- and left-moving waves as the length of the cell l is changed with other parameters fixed. In all cases the right-moving waves A_R dominate. For the upper figure $s=1.7$, and for the lower figure $s=2.2$. Other parameters were $g=4, \alpha=\beta=-0.06$.

This tends to $(g-1)/(g+1)$ for large s. For the parameters of Fig. 3 Eq. (11) gives $l_R/l \simeq 0.4$, consistent with the numerical result. The filling to confined transition is not sharp, as shown in Fig. 5. Note that the confined solutions for s somewhat greater than 2 may become unstable to periodic modulation: this is discussed below.

B. Defect solutions

Two types of defects are characteristic of one-dimensional nonlinear waves: targets are patterns in

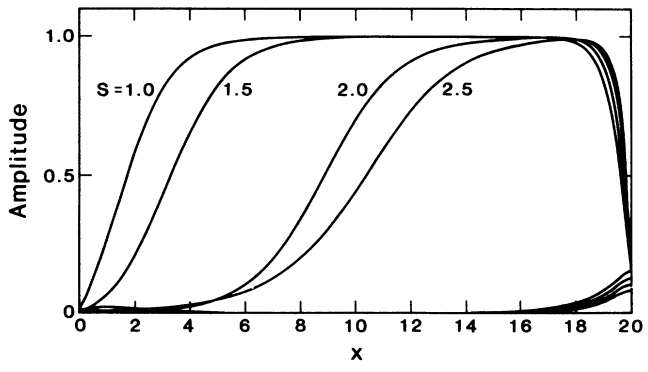

FIG. 5. Transition between steady-state solutions corresponding to filling states for $s<2$ and confined states for $s \gtrsim 2$. The parameters used were $l=20$, $g=4$, and $\alpha=\beta=-0.06$.

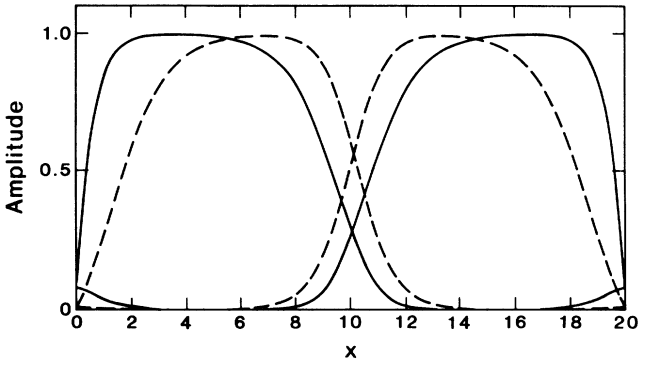

FIG. 6. Steady-state solutions for targets (solid line)—waves moving away from the central point—and shocks (dashed line)—waves approaching the central point. Parameters used were $l=20$, $s=1.0$, $g=4$, and $\alpha=\beta=-0.06$. The target solution is unstable to small off-center perturbations.

which waves emanate from a region of reduced amplitudes and shocks are the reverse, where waves approach a point from opposite directions. In the system where states with wave vector k and $-k$ are disconnected (in the absence of strong perturbations such as amplitudes changing to zero) these defects have a topological character in an infinite region. Both types of defects may be found as illustrated in Fig. 6, most easily at small s and large l. The shock solution in Fig. 6 is shown to be stable to small perturbations by the dynamic simulations, but the target solution is unstable on a long time scale to moving towards one end wall. For large l and $s \gtrsim 2$ the targets are more rapidly unstable to the region of right- (left-) moving waves propagating away to the right (left), initially leaving a growing quiescent region. In finite boxes the confined states are ultimately reached.

IV. DYNAMIC EVOLUTION

Equations (8)–(10) were evolved in time using a finite difference scheme and implicit evolution of the linear terms with explicit treatment of the nonlinear terms, both second order accurate in time. Typically 80 to 160 spatial mesh points for each of A_R and A_L were used, with time stepping of 0.01 to 0.1.

The main results to be described are the evolution of the dynamics as s is increased for fixed l. The sequence of behavior typically observed is as follows: stationary filling→stationary confined→modulated confined →asymmetric oscillations→symmetric oscillations →asymmetric oscillations→asymmetric stationary. However, the behavior does depend on l, with for example the oscillatory behavior becoming less evident at smaller l. Remembering[5] that the zero-amplitude state becomes stable for $l/s \lesssim |\ln r|$ with r the reflection coefficient, we can identify the final spatially symmetric stationary state with a weak nonlinear saturation of the linear transient observed by Kolodner *et al.*,[8] and in these numerical solutions. For a fixed s, larger l is equivalent to stronger nonlinearity.

A. $l=10$

An initial condition of a small Gaussian envelope of right-moving waves with maximum amplitude 10^{-10} and standard deviation 0.5 about $x=5$ was used, with values of $s=1$, 2, 3, and 4. In these cases a steady state was always reached at long times. The transient initial evolution of the amplitude functions paralleled the observations of Kolodner *et al.*,[8] reaching an exponentially growing but nonoscillatory state with symmetric amplitudes of right-moving waves large at $x>0$, and left-moving waves large at $x<0$ with characteristic exponential spatial envelope, as discussed in Ref. 5. The final steady-state solutions are shown in Fig. 7. The sequence follows the general trend, except oscillatory final states are absent, although oscillating transients corresponding to small modulations of the confined state are clearly seen for $s=2$. For $s=4$ the final symmetric state appears as a nonlinear saturation of the symmetric growing transient. This solution corresponds to the weak nonlinear solution of Zaleski *et al.*,[12] although they did not realize that their results are valid only for small s (group speed) as discussed above.

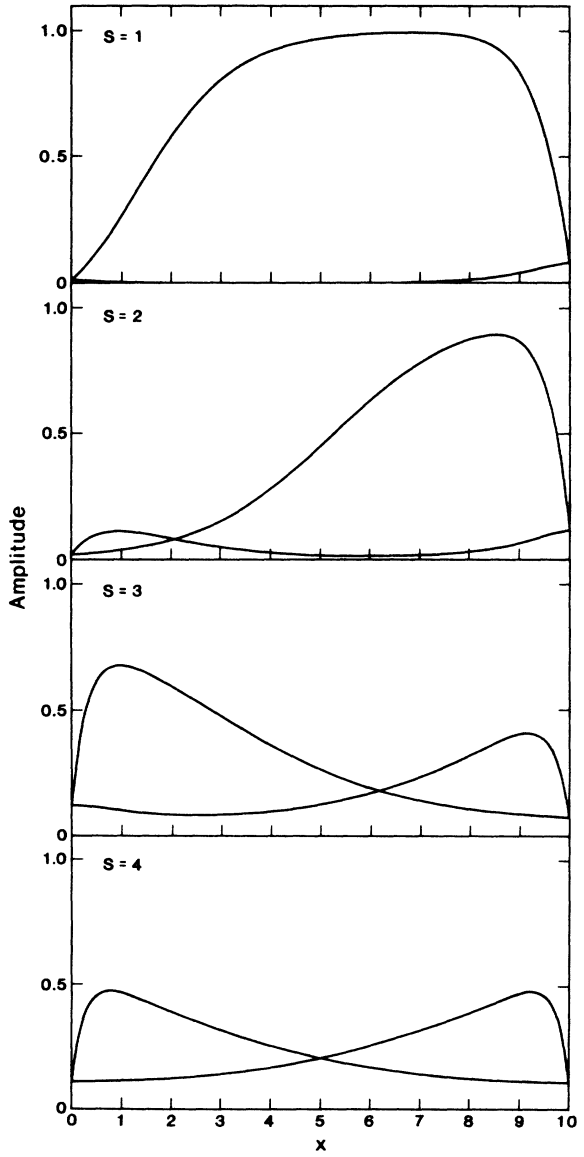

FIG. 7. Final steady states evolving from a small localized initial condition for $l=10$ and various values of s. Other parameters are $g=4$ and $\alpha=\beta=-0.06$.

B. $l=20$

For small s both filling solutions and solutions with defects (cf. Fig. 6) were found, depending on the initial conditions. At $s=2$ a confined stationary state is seen. Increasing s slightly beyond this value (e.g., 2.05) gave a persistent oscillation with period about 41, rather greater than the cell transit time $2l/s\sim 19.5$ [Fig. 8(a)]. The oscillation corresponds to a small to-and-fro oscillation of the position where the amplitude rapidly grows, or equivalently to a modulation of the amplitude of the pattern concentrated in the middle portion of the cell. In terms of the original variables this motion would be quasiperiodic, and an amplitude modulation of the waves. The amplitude of the modulation grows as s is increased, and the period drops. For example, at $s=2.5$ a considerable amplitude of left moving waves is seen at the left end of the cell for half the period [Fig. 8(b)]. The period is about 28, so is dropping more rapidly than s^{-1}. Beyond $s=2.8$ symmetric oscillations are seen, with large ampli-

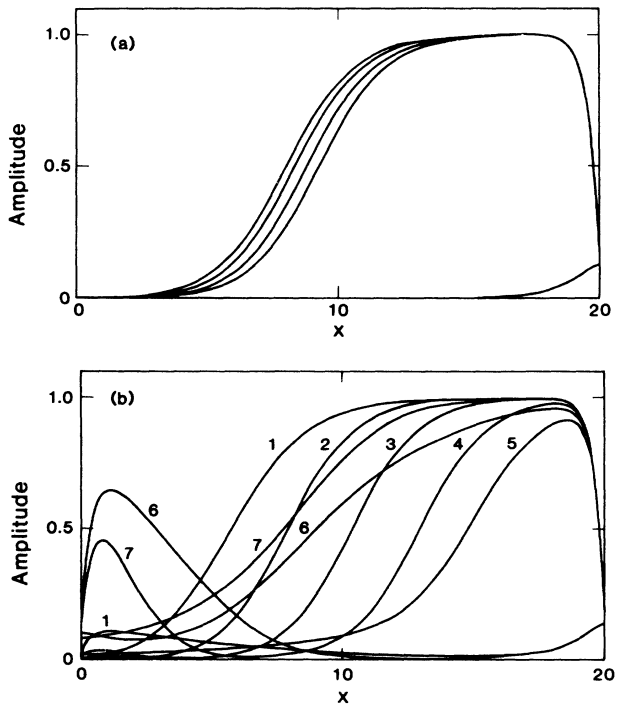

FIG. 8. Periodic dynamic solutions for $l=20$ and (a) $s=2.05$ and (b) $s=2.5$. The amplitudes are plotted for a sequence of equally spaced times. In both cases right-moving waves dominate, but appreciable amplitudes of left-moving waves are seen at times 6 and 7 in (b). Other parameters as in Fig. 7.

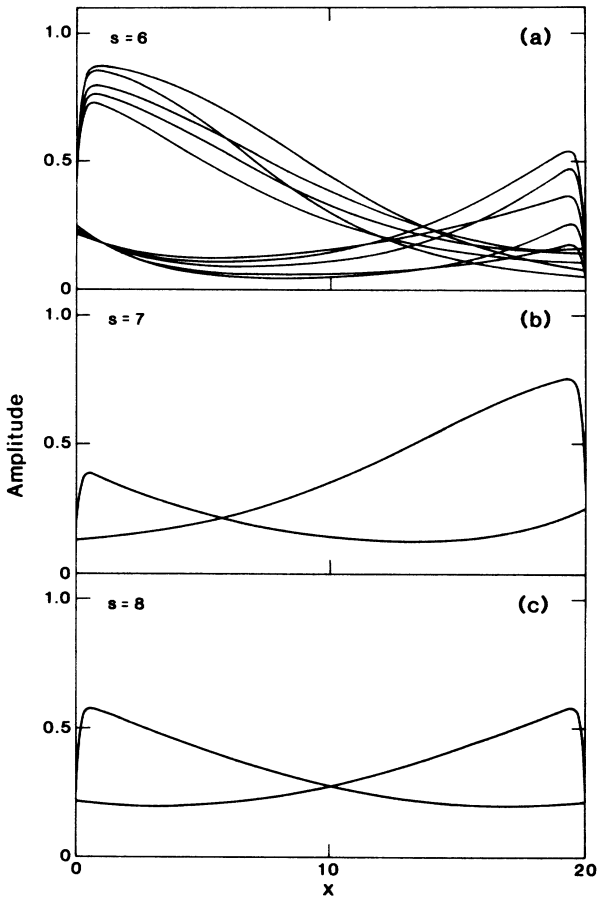

FIG. 9. Dynamic solutions for $l=20$ and (a) $s=6$, (b) $s=7$, and (c) $s=8$. For $s=6$, the motion is periodic and the amplitudes were plotted at equally spaced time intervals. Left-moving waves dominate in this run. For $s=7$ (b) shows a stationary solution with dominant right-moving waves. At $s=8$ a stationary state with equal amplitude right-moving waves in the right end and left-moving waves in the left end is seen.

tude right-moving waves concentrated at the right end of the cell replaced half a period later by equal amplitude left-moving waves at the left end of the cell. The period increases considerably (period 51 at $s=2.9$). As s increases further the period decreases again, and the amplitudes become asymmetric as ξ_L becomes comparable to the length of the system [Fig. 9(a)]. Further increase in s yields a stationary asymmetric state [Fig. 9(b)] and by $s=8$ a stationary symmetric state as above [Fig. 9(c)].

V. COMPARISON WITH EXPERIMENT ON BINARY FLUID CONVECTION

Confined states reminiscent of Fig. 3(b) have been observed in experiments on binary fluid convection by Moses *et al.*[6] and Heinrichs *et al.*[7]—flow visualization was used, so that no quantitative information on the spatial dependence of the flow is available. As discussed above, since the transition to oscillatory convection in these experiments is discontinuous, giving a jump to finite amplitude states which theoretically are anticipated to have rather complicated structure, the small amplitude approach pursued here is not quantitatively applicable. Nevertheless we may attempt to get some understanding of the experiment. Qualitatively many features are reproduced. The important parameter in the theory of the filling-to-confined transition is $\bar{s}\sim s/\epsilon^{1/2}$. Based on the results of Ref. 3 (cf. Fig. 2), that the heat convected by the slowly travelling nonlinear states is quite accurately given by $N_p(\epsilon_p)$ with $\epsilon_p=(R-R_{cp})/R_{cp}$ and R_{cp} and N_p the critical Rayleigh number and Nusselt number function for pure stationary convection, we may estimate ϵ by ϵ_p. The observed speed in Ref. 3 decreases with increasing ϵ_p: thus increasing $\bar{s}$ should correspond to decreasing ϵ_p. From the results of the present work we would expect to see filling states for large ϵ_p, with a transition to confined states as ϵ_p decreases. This is indeed found experimentally. We can roughly estimate from the data the value of $\bar{s}$ at the transition, using

$$\bar{s}=\left[\frac{\Omega}{\Omega_c}\right]\frac{s_0\tau_0}{\xi_0}\epsilon_p^{-1/2}\,, \tag{12}$$

with Ω the observed frequency of the waves at the transition and Ω_c the frequency at the linear onset s_0 the group speed at onset, and ξ_0,τ_0 the parameters of the amplitude Eq. (2). In Eq. (12) the measured change in the phase speed Ω/Ω_c is used to estimate the change in the group speed s/s_0, which was not measured. The data of Fig. 1 of Ref. (7) is for fluid parameters Prandtl number 18, Lewis number 0.015, and separation ratio -0.12. For these values theoretical calculations[16] give $s_0\simeq 2.3$, and we use the values for pure stationary convection at Prandtl number 18: $\xi_0\simeq 0.38, \tau_0\simeq .053$. Also, at the transition ϵ_p may be estimated from Fig. 1 of Ref. 3 to be about 0.04, and Ω/Ω_c is about 0.5 in the confined state at a somewhat different value of ϵ_p. These values give $\bar{s}\sim 0.8$, perhaps in reasonable agreement with the expected value of 2 considering the crudeness of the estimate.

In addition Heinrichs *et al.* observe confined states that have a slow periodic amplitude modulation. These states may be associated with the modulated confined states predicted here, although Heinrichs *et al.* discuss an alternative explanation due to Knobloch.[17]

Other qualitative features of the experiments[6,7] require further consideration. It is not clear if the reduced Nusselt number observed in the confined states is simply due to the reduced region of convection, or if the heat current in the saturated region is also suppressed. The observed transition to the filling state is apparently discontinuous, whereas the transitions in the amplitude equations are continuous, although they occur over quite small changes in the parameters. It would be interesting to look for the more dramatically oscillating states predicted here for increasing $\bar{s}$ and system size; there are some preliminary results along these lines.[18] There is also numerical evidence for such states in simultations of the fluid equations between free-slip pervious top and bottom plates but rigid end walls.[19]

Thus there is considerable qualitative success of the simple theory presented here. A more complete comparison with experiment clearly requires a better understanding of the nonlinear states. It is clear, however, that quite complicated spatial and temporal effects may arise simply from the combination of propagation and the finite geometry, even before we allow for the possibility of exotic instabilities.

Note added in proof. Since the submission of this paper, oscillating states similar to the ones predicted Sec. IV B have been described by Fineberg, Moses, and Steinberg[20] and Kolodner and Surko.[21] Also Croquette and Williams[22] have observed the transition from a symmetric stationary state to an asymmetric stationary state similar to the one shown in the lower two panels of Fig. 7 near the transition to the oscillatory instability for straight rolls in pure fluid convection.

[1]T. B. Benjamin and J. E. Feir, J. Fluid Mech. **27**, 417 (1966); A. C. Newell, *Lectures in Applied Mathematics*, (American Mathematical Society, Providence, 1974), Vol. 15, p. 157.
[2]H. R. Brand, P. S. Lomdahl, and A. C. Newell, Physica **23D**, 345 (1986).
[3]C. M. Surko, P. Kolodner, A. Passner, and R. W. Walden, Physica **23D**, 220 (1986).
[4]R. J. Deissler, Physica **25D**, 233 (1987).
[5]M. C. Cross, Phys. Rev. Lett. **57**, 2935 (1986).
[6]E. Moses, J. Fineberg, and V. Steinberg, Phys. Rev. A **35**, 2757 (1987).
[7]R. Heinrichs, G. Ahlers, and D. S. Cannell, Phys. Rev. A **35**, 2761 (1987).
[8]P. Kolodner, A. Passner, C. M. Surko, and R. W. Walden, Phys. Rev. Lett. **56**, 2621 (1986).
[9]P. Coullet, S. Fauve, and E. Tirapegui, J. Phys. (Paris) Lett. **46**, 787 (1985).
[10]A. C. Newell, Ref. 1.
[11]M. C. Cross, Phys. Fluids **25**, 936 (1982).
[12]S. Zaleski, P. Tabeling, and P. Lallemand, Phys. Rev. A **32**, 655 (1985).
[13]D. G. Aronson and H. F. Weinberger, Adv. Math. **30**, 33 (1987).
[14]E. Ben-Jacob, H. Brand, G. Dee, L. Kramer, and J. S. Langer, Physica **14D**, 348 (1985).
[15]P. Coullet, C. Elphick, L. Gil, and J. Lega, Phys. Rev. Lett. **59**, 884 (1987).
[16]M. C. Cross and K. Kim, Phys. Rev. A **37**, 3909 (1988).
[17]E. Knobloch, Phys. Rev. A **34**, 1538 (1986).
[18]C. M. Surko (private communication).
[19]A. E. Deane, E. Knobloch, and J. Toomre (unpublished).
[20]J. Fineberg, E. Moses, and V. Steinberg, Phys. Rev. Lett. **61**, 838 (1988).
[21]P. Kolodner and C. M. Surko, Phys. Rev. Lett. **61**, 842 (1988).
[22]V. Croquette and H. Williams (unpublished).